Journal of Marine Research, 49, 379–401, 1991

Early diagenesis of chlorophyll-*a* in Long Island Sound sediments: A measure of carbon flux and particle reworking

by Mingyi Sun[1], Robert C. Aller[1] and Cindy Lee[1]

ABSTRACT

Sedimentary chlorophyll distributions reflect supply from primary production in overlying waters, transport during sedimentation/bioturbation, and alteration due to decomposition/transformation reactions. In Long Island Sound sediments, seasonal depth profiles of chlorophyll-*a* (Chl-*a*) often decreased exponentially within a few centimeters of the sediment-water interface, implying that initial decomposition rates of Chl-*a* were faster than surface sediment mixing rates. The highest surface sediment concentrations of Chl-*a* occurred in early spring, shortly after the spring bloom; the lowest concentrations occurred in summer. Chl-*a* was more concentrated at the shallow station (~15 m) than at the deeper station (~40 m) implying greater water column degradation or generally lower supply to deeper regions. Anoxic incubation experiments revealed that the degradation of Chl-*a* in fresh sediment apparently involves at least two stages. We operationally defined two pools of Chl-*a* as "free" and "bound" by their ease of extraction using a freeze-thaw technique. Thus, we hypothesized for the sake of a mathematical model that an initial degradation stage exists where Chl-*a* is released from a bound state, and a second stage where the released Chl-*a* degrades. These processes can be described by first-order kinetics ($k_r = 0.14 - 0.19$ d^{-1} and $k_d = 0.02 - 0.04$ d^{-1}). The release rate is larger than the degradation rate, so that the release process dominates initial degradation behavior. Bound Chl-*a* may also degrade before being released. A simple, one-dimensional transport-reaction model shows that the largest Chl-*a* fluxes occurred in spring and the smallest in summer, while higher particle mixing rates occurred in summer than spring. Sediment mixing coefficients (D_B) calculated using Chl-*a* profiles are roughly comparable with those estimated from ^{234}Th distributions, and estimated carbon fluxes agree reasonably well with total benthic O_2 uptake.

1. Introduction

Primary production by phytoplankton in surface waters is a major source of labile organic carbon to coastal sediment. Particles from the euphotic zone sink to the sediment-water interface, where benthic organisms rapidly degrade the labile organic compounds present in the settled materials. The rate and extent of organic matter degradation significantly affect the chemistry of marine sediments (Berner, 1980). Chl-*a* is the most abundant pigment component in almost all species of phytoplankton. Degradation products are mostly formed by a variety of herbivorous

1. Marine Sciences Research Center, SUNY, Stony Brook, New York 11794, U.S.A.

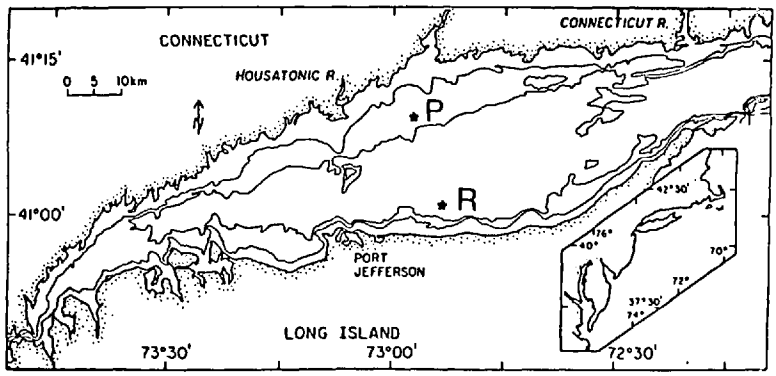

Figure 1. Long Island Sound study site. Stations P and R are both located in muddy sediments.

grazing activities by microzooplankton and macrozooplankton in the water column (Shuman and Lorenzen, 1975; Hallegraeff, 1981; Welschmeyer and Lorenzen, 1985) or benthic filter-feeders and deposit-feeders in sediments (Gelder and Robinson, 1980; Hawkins *et al.,* 1986; Bianchi *et al.,* 1988). The concentration of Chl-*a* is commonly used to estimate water column phytoplankton biomass, while the concentrations of its degradation products (phaeopigments) are used as diagnostic indicators of physiological status, detrital content and grazing processes in natural populations of phytoplankton (Mantoura and Llewellyn, 1983). Open ocean sediments generally contain little or no Chl-*a* because most Chl-*a* degrades in the deep water column unless surface water productivity is unusually high (SooHoo and Kiefer, 1982; Cole *et al.,* 1985; Graf, 1989). In contrast, Chl-*a* can be found commonly in nearshore and shelf sediments due to relatively higher primary production and comparatively less complete degradation in the water column (Montagna *et al.,* 1989; Banta *et al.,* 1990; Rabalais and Turner, 1990).

If the degradation rates of sedimentary Chl-*a* were known, then in principle, the distribution and abundance of Chl-*a* in surface sediments could be used to estimate delivery of planktonic debris to the sea floor and investigate sedimentary processes such as particle reworking. In this paper, we examine this potential at two muddy sites in Long Island Sound, an estuarine embayment along the NE coast of North America. Experimental studies of sedimentary Chl-*a* degradation are combined with field measurements of Chl-*a* distribution in a diagenetic model used to quantify seasonal changes in organic carbon flux and particle bioturbation in central Long Island Sound (LIS).

2. Methods

a. Study sites. Two stations (P and R) representing two different depositional environments in central Long Island Sound were chosen for this study (Fig. 1). These

stations are from the same location as two previously well-studied LIS sites (NWC and DEEP) for which hydrographic and biological features were described by Yingst and Rhoads (1978) and Aller (1980). Briefly , the depth of the water column is 15 m at station P and 40 m at station R. The average sedimentation rates at both stations range between 0.02–0.06 cm/yr. Station P is subject to constant resuspension of the top 1 mm of surface sediment, while the upper few centimeters may be eroded and redeposited during major storms (Aller and Cochran, 1976; McCall, 1978). Station R sediments are also subject to resuspension, but mostly through tidal scour rather than storm resuspension; turbidity there is considerably lower than at station P. The bottom fauna in central Long Island Sound have distinct distributions which are related to differences in depth, depositional environment, and the severity and frequency of physical disturbances (McCall, 1977). Station P has a relatively stable, low-diversity assemblage of organisms characterized by large numbers of deep-feeding deposit feeders such as the highly active protobranch bivalves *Yoldia limatula* and *Nucula annulata,* and the errant polychaete *Nephtys incisa.* Permanent tube-dwelling polychaetes are not common, but the infaunal anemone, *Ceriantheopsis americanus,* is plentiful. Polychaetes at station R form permanent dwelling tubes and are generally larger, more sedentary, and burrow deeper than at station P. Both stations P and R are subject to sinusoidal variations in surface water temperature during the year ranging from about 2°C in February–March to about 22°C in August–September (Riley, 1956).

Surface sediment samples were also taken from Flax Pond, a shallow embayment on the north shore of Long Island (Woodwell and Pecan, 1973). Seasonal organic matter decomposition rates in Flax Pond sediments encompass nearly the entire range of rates commonly found in nearshore sediments and marshes (Mackin and Swider, 1989).

b. Sampling. Sediment cores from LIS were collected seasonally using a Soutar-style box corer (surface area $\sim 25 \times 25$ cm). After retrieval of the box core, sub-cores of 10–20 cm length were taken by gently pushing core tubes or rectangular acrylic corers into the sediment. Rectangular subcores were first X-rayed for sediment structure and subsequently sliced, as were tube cores, into 0.5–1 cm intervals (upper 5 cm depth) or into 2–3 cm intervals (below 5 cm depth). Any effects on core depth due to compression were ignored. All subsamples were stored frozen until extraction. Sampling was carried out during May, August and October, 1988, and February and April, 1989. Flax Pond samples were collected by scraping the top 1 cm from surface sediments.

c. Experimental design. Surface sediment samples for use in a variety of mixing and decomposition experiments were taken from LIS station P and from intertidal sediments adjacent to *Spartina* marsh areas in Flax Pond. Decomposition experi-

ments consisted of monitoring Chl-*a* concentrations as a function of time in a series of anoxically-incubated sediment samples. In most cases, sediment was first homogenized by hand-mixing in a nitrogen-filled glove bag (no additional water added); subsamples were then placed in small screw cap jars and stored in a N_2 flushed container. In one set of experiments (20°C), the effect of physical mixing on degradation patterns was examined by comparing a series of mixed and unmixed surface core sections (0–2 cm) placed into incubation jars. These sediments were never frozen, either before incubation or before extraction.

Three basic types of decomposition experiments were carried out: (1) fresh sediment samples which had never been frozen were incubated at two different temperatures (4°, 20°C) in the dark under flowing nitrogen; individual samples were removed at various times for extraction; (2) sediment was first frozen at −70°C and then thawed before beginning the incubation period (at 20°C); samples were then removed at various times for extraction; (3) fresh sediment was incubated as above at three temperatures (5°, 15°, 25°C) and then frozen at −70°C and thawed prior to extraction. These experiments were designed to investigate whether Chl-*a* was present in different forms within the sediments studied here. It has been shown that the degradation of organic compounds in both seawater and sediments can depend on the particular matrix the compound is associated with as well as its structural characteristics (Wakeham and Lee, 1991). Our initial experiments and those of previous investigators (Repeta and Gagosian, 1987; Downs, 1989) have suggested that Chl-*a* and other pigments can be associated with a variety of sediment matrices, e. g., intact cells, fecal pellets, or amorphous detritus. To extract Chl-*a* from such matrices can require techniques of varying degrees of harshness. Measurement of overall rates of degradation may best be accomplished by extracting as much of the Chl-*a* as possible, but this approach loses potential information gained from stepwise extraction about the various forms of Chl-*a*. Thus, we used a freeze-thaw technique to differentiate between Chl-*a* bound to the sediments in varying degrees.

d. Pigment analyses. Pigments were extracted from thawed wet sediments using glass-distilled 100% acetone. Absolute acetone (100%) was used instead of the 90% commonly used in water-column particle analysis to avoid any artifactual production of chlorophyllide (Jeffrey and Hallegraeff, 1987). Sediment subsamples (~ 1 g) were mixed using a vortex stirrer with 5 ml acetone and sonicated for 10 min. The acetone extract was separated from the sediment by centrifugation at 3000 rpm for 5 min and decanted. Each subsample was extracted twice; a third extract usually contained less than 1% of the total pigment content. The ratio of sediment weight to solvent volume was optimized to achieve maximum recovery with a minimum solvent use. Combined extracts were filtered through 0.2 μm Zetapor® membrane filters and stored at −15°C prior to pigment analysis, generally within one day. In order to avoid

photodegradation of pigments, sample extractions were carried out under subdued yellow light.

Some extraction methods may convert Chl-*a* into degradation products or colorless residues. For example, when we used a two step acetone/ether/pentane extraction method on LIS sediment samples (Furlong and Carpenter, 1988), we observed almost no Chl-*a* but higher phaeopigment concentrations than by the simple acetone extraction method. Chl-*a* appeared to be sensitive to degradation during the ether evaporation step used in this method. A simple 100% acetone extraction may be one of the more efficient methods to remove pigments from sediment and may reduce degradation artifacts (Keely and Bereton, 1985; Jeffrey and Hallegraeff, 1987).

Pigment concentrations were determined by ion-pairing reverse-phase high performance liquid chromatography (Mantoura and Llewellyn, 1983). The HPLC system used consisted of a Beckman Model 420 gradient controller with Beckman 110 pumps. Columns used were either a 5 μm C-18 (ODS) Alltech column (250 mm × 4.6 mm i.d.) or a 5 μm C-18 Adsorbosphere column (250 mm × 4.6 mm i.d.). Detection was accomplished with a Kratos FS 970 fluorometer using an excitation wavelength of 405 nm and measuring emission at >580 nm and with a Kratos UV absorbance detector using a wavelength of 377 nm (Furlong and Carpenter, 1988). Results were integrated by a Shimadzu C-R3A Chromatopac. Mobile phases used in the gradient elution consisted of a primary eluant (80% methanol; 20% aqueous solution of 0.5 mM tetrabutyl ammonium acetate and 10 mM ammonium acetate) and a secondary eluant (20% acetone in methanol). After injection (50 μl extract), a gradient program ramped from 100% A to 100% B in 15 min with a hold for 60 min, providing sufficient resolution of all pigments of interest. All chromatographic separations were performed at room temperature at a flow rate of 1.0 ml/min.

Identification of Chl-*a* in the sediment samples was confirmed by co-elution with an authentic standard. Authentic Chl-*a* was obtained from Sigma Chemical Co. and was quantified spectrophotometrically (Hewlett Packard 8452 A Diode Array Spectrophotometer) using an extinction coefficient of 68,700 at 440 nm (Mantoura and Llewellyn, 1983). Peak areas were converted to concentrations using response factors calculated using the authentic standard. Replicate HPLC measurements of pigment standards (over a few months) and sediment extracts varied by ±10%. Recovery of standard Chl-*a* added to wet sediments was 90.6 ± 3.1% (by fluorescence) or 102.1 ± 6.0% (by UV). Concentrations reported here are based on fluorometric peak areas. Chl-*a* concentrations are reported in units of nmol/cm^3, corrected for porosity as measured by water content.

3. Results

a. Seasonal profiles. The concentrations of Chl-*a* in Long Island Sound surface sediments (0–1 cm) varied with season and sample site (Table 1). In general, two distinct features can be seen in the surface concentrations: (1) spatially, the shallow

Table 1. The concentration of Chl-*a* (nmol/cm^3) in LIS station P and R surface (top 1 cm) sediment.

Station	May-88	Aug-88	Oct-88	Feb-89	Apr-89
Sta. P	4.74	0.88	0.60	9.16	11.7
Sta. R	2.03	0.77	0.76	3.85	1.82

water station P had higher concentrations of Chl-*a* than the deeper water station R; and (2) seasonally concentrations of Chl-*a* were higher in late winter-spring than in summer and fall. More extensive spatial and temporal surveys conducted in LIS (unpublished data) confirm these as general patterns. The concentrations of Chl-*a* also varied markedly with sediment depth at each site (Fig. 2a, 2b) Concentrations often decreased exponentially at both sites below the sediment-water interface. For Chl-*a*, the concentration gradient with depth was large in early spring (FEB), decreasing rapidly from high surface concentrations to 1–2 nmol/cm^3 within the top 2 cm. Later, in April and more so, in May, the Chl-*a* gradients were still large, but the surface concentration was lower and labile Chl-*a* penetrated deeper (about 5 cm depth). During summer (AUG) and fall (OCT), the surface concentrations of Chl-*a* were very low; depth profiles showed more scatter; and a subsurface maximum at a few cm depth was sometimes present. Averaged porosity profiles from May 88 to April 89 are shown in Figure 3. Integrating Chl-*a* concentrations over the top 10 cm resulted in the seasonal inventories shown in Figure 4.

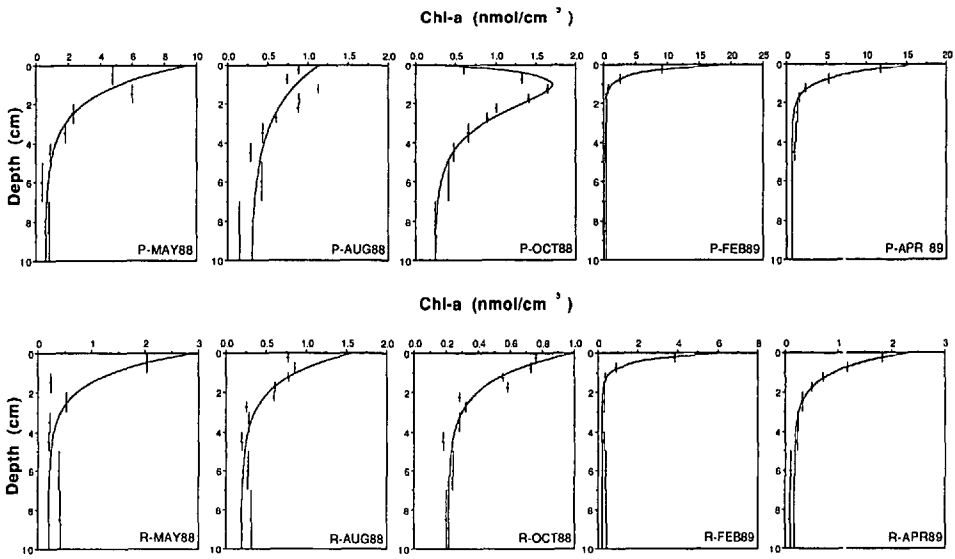

Figure 2. (a) Chl-*a* concentrations in depth profiles from Station P; (b) Chl-*a* concentrations in depth profiles from Station R. Lines are fits to the data by the diagenetic model (except the profile at Station P in OCT 88 where the line is added to aid comparison of data).

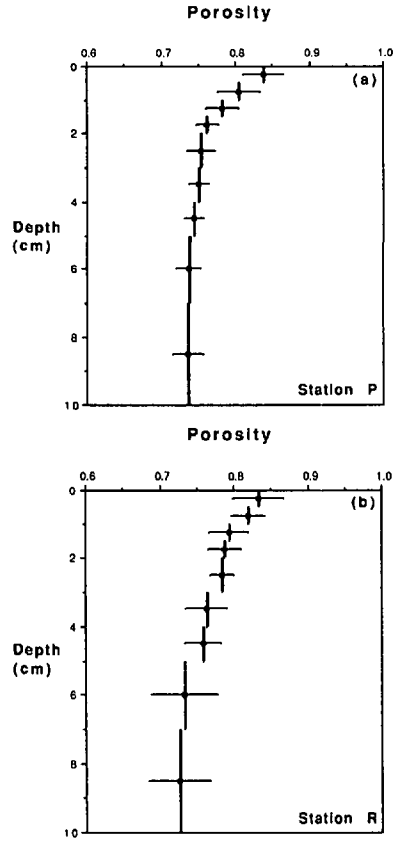

Figure 3. (a) Porosities in depth profiles from Station P; (b) Porosities in depth profiles from Station R. Horizontal lines are seasonal deviations between the 5 sampling periods.

b. Decomposition experiments. Because Chl-*a* is the major sedimentary phorbin and the primary source for degradation products, it is emphasized here as an indicator of chloropigment diagenesis. During anoxic incubation experiments with fresh surface sediments from LIS station P and Flax Pond, Chl-*a* concentrations increased initially to a maximum before beginning to decrease after about 1 week (Fig. 5a and 5b). Figure 5a shows the results of incubations at two different temperatures (4°C and 20°C) while Figure 5b shows the results of incubations of mixed and unmixed sediments at 20°C. There was very little difference in the pattern of Chl-*a* concentration over time between the two temperatures or between the mixed and unmixed sediments. Chl-*a* concentrations in similar incubation experiments in Flax Pond sediments at 5°, 15°, and 25°C also showed no temperature dependence.

When fresh sediment was frozen at ~ -70°C before incubation, the measured Chl-*a* concentration was higher than in previously unfrozen fresh sediment (shown in Figure 5b as initial frozen sediment). When samples were frozen after rather than

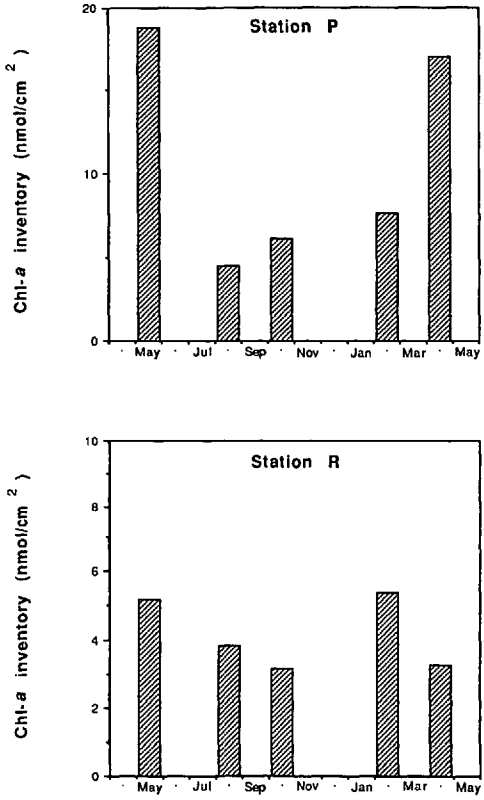

Figure 4. Inventory of Chl-*a* in the upper 10 cm between May, 1988 and April, 1989.

before extraction, a nearly equivalent differential amount of Chl-*a* was released. The amount of Chl-*a* released varied with season; higher values occurred in early spring (FEB) and lower values in late spring and summer (MAY and JUN). This implies that part of the Chl-*a* may exist in intact cells or in a matrix which can resist extraction by organic solvents, as discussed previously. Freezing can apparently break down this binding mechanism and increase extraction efficiency. Results from incubating previously frozen samples are shown in Figure 6. The Chl-*a* concentration in this case decreased from the beginning of incubation; however, this decrease lasted only a few days before a constant concentration was reached. When fresh samples were incubated and then frozen and thawed just before extraction, initial increases in extracted Chl-*a* during the first week were subdued or absent compared with fresh sample incubations within a pre-extraction freezing step. Incubations at different temperatures again showed little or no difference in degradation pattern.

Simultaneous measurements of pore water $SO_4^=$ (measured gravimetrically using $BaSO_4$) and sediment Chl-*a* during the incubation of Flax Pond sediment are shown in Figure 7. Sulfate decreased continuously, presumably due to sulfate reduction

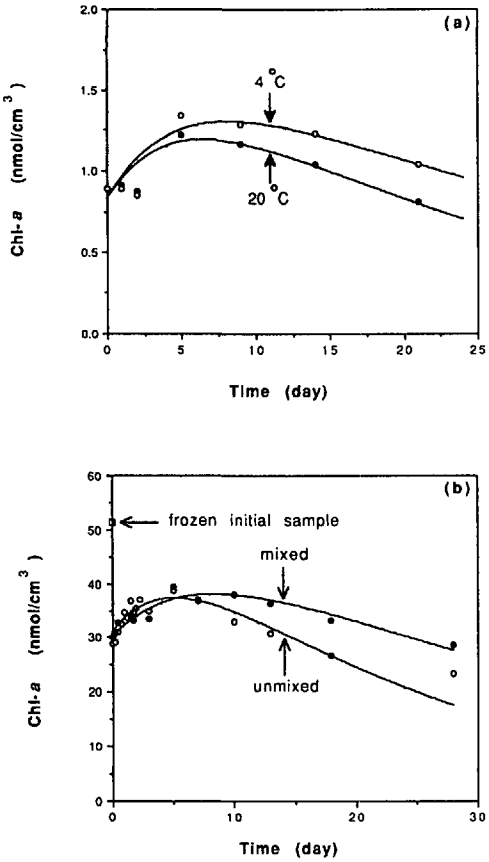

Figure 5. Chl-*a* concentrations in fresh sediments as a function of time during anoxic incubation: (a) Station P sediment at two different temperatures; (b) Flax Pond sediment, 20°C, mixed and unmixed. The lines are fits to data by the degradation model (Eq. 4a). Note the concentration of extractable Chl-*a* in the frozen sample.

during the various stages of increasing extractable Chl-*a* and subsequent Chl-*a* decrease. Chl-*a* continued to decrease after total depletion of $SO_4^=$ (about 17 d). As is commonly observed, $SO_4^=$ depletion is initially zero order at higher $SO_4^=$ concentration, but becomes first order at concentration ranges less than ~2–5 mM (e.g., Ramm and Bella, 1974).

4. Discussion

a. Spatial and seasonal patterns of sedimentary Chl-a. No significant benthic photosynthesis occurs at the stations examined in this study because of the relatively high turbidity in the water column. Thus, the source of Chl-*a* in sediments is related directly to primary production in overlying surface waters and the delivery of

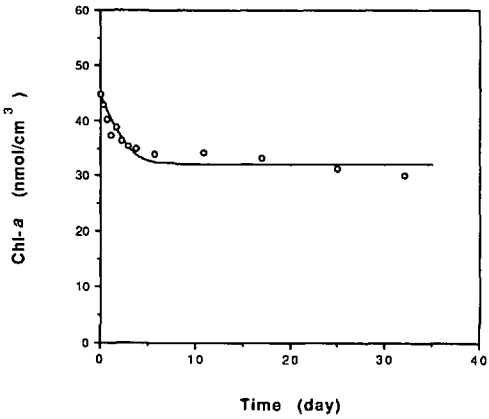

Figure 6. Concentration of Chl-*a* in sediments which were first frozen and then thawed before incubation. The line is added to aid comparison of data.

planktonic debris to the sediment surface. In Long Island Sound, as in many temperate regions, net phytoplanktonic production follows a relatively regular seasonal pattern with a maximum in late winter-spring and a smaller secondary fall maximum (Conover, 1956). The inventories of Chl-*a* in surface sediment (upper 10 cm) follow this pattern and have the highest values in spring when net supply is high and the lowest values in summer-early fall when heterotrophic metabolic activity is relatively high and pigment production is low (Fig. 4).

In general, Chl-*a* flux to the sea floor should decrease with an increase in water depth because of the longer time for degradation to occur in the water column. Variations in flux may also be due to small-scale spatial differences in primary production in the Sound or to variable resuspension processes between the two

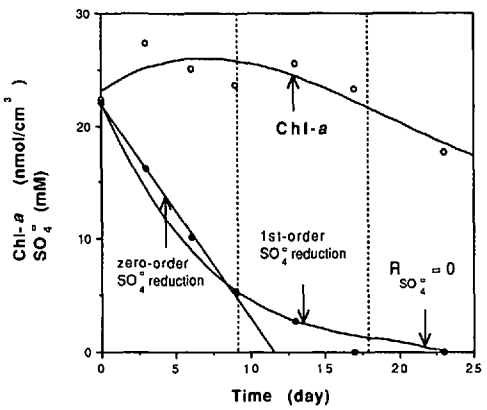

Figure 7. Changes in the concentration of Chl-*a* and $SO_4^=$ with time during the incubation of Flax Pond fresh sediment. The curve for Chl-*a* data is derived from the degradation model (Eq. 4a); the curve for $SO_4^=$ represents the fit to a 1st-order degradation model; the straight line for $SO_4^=$ represents the fit to a zero-order degradation model.

stations. These latter processes were not evaluated here. In this study, surface samples from shallow station P have higher inventories of Chl-*a* than at deeper station R. Assuming there are no major differences in sediment degradation rates, these differences must reflect differences in supply to and incorporation into the sediment deposits. The proximity of the two stations in the central Sound implies that overlying primary production is similar so that inventory differences are most likely due to differences in water column depth or surface sediment degradation and circulation patterns.

Some insight into the likely processes controlling Chl-*a* inventories can be derived from the distribution of excess ^{234}Th in bottom sediments. This natural radionuclide is produced continuously by uranium decay in the water column and, in Long Island Sound, is rapidly and completely scavenged onto particles. It decays on a timescale ($t_{1/2}$ = 24.1 day) similar to that of Chl-*a* (see discussion below). In a simple particle sedimentation cycle, excess ^{234}Th sedimentary inventories would be proportional to the amount of uranium in the overlying waters, and therefore to water column depth. However, in Long Island Sound, ^{234}Th inventories are highest in shallow water sediments and, in particular are higher at station P than R. This is the opposite of that expected simply on the basis of vertically overlying uranium source (Aller *et al.*, 1980; Cochran *et al.*, unpublished). Differential scavenging of advected fluid over different areas cannot explain the inventory pattern as there are no detectable spatial gradients in dissolved ^{234}Th, and mixing of LIS water occurs over a much longer timescale (10–14 d) than ^{234}Th residence time ($\leq$1–2 d). Because long-term net sedimentation rates are not greatly different at P and R, Aller *et al.* (1980) suggested that suspended particles formed in the water column are initially exchanged into rapidly bioturbated muddy regions and can then be transported through successive resuspension-particle exchange to more slowly bioturbated deeper regions such as R where exchange occurs more slowly, presumably after significant degradation of the most reactive components (e. g., decay of ^{234}Th) has taken place. This model is consistent with ^{210}Pb inventory patterns (Turekian *et al.*, 1980). The average C/N ratio of decomposing organic matter is higher in the upper 10 cm of sediment at R than at P also implying the delivery of a more degraded material to the deeper region (Aller and Yingst, 1980; Aller and Benninger, 1981). The Chl-*a* inventory patterns documented here (Fig. 4) are consistent with both the ^{234}Th inventory and decomposition data, assuming overlying primary production is not greatly different in the two areas. This also suggests the use of Chl-*a* as a useful adjunct to ^{234}Th as a tracer of reactive particle dynamics in comparable environments.

b. Chl-a degradation rates. Interpretation of the Chl-*a* distributions requires knowledge of the rates and mechanisms of degradation. Previous studies have shown that Chl-*a* in algae and higher plant debris degrades over characteristic timescales of several weeks (Bianchi and Findlay, unpublished). Both the rate and the mechanism

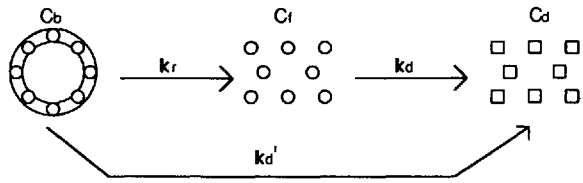

Figure 8. Conceptual representation of Chl-*a* degradation in fresh anoxic sediments. C_b, C_f, and C_d represent bound (possibly but not necessarily in cell components), free, and degraded (derived from both bound pool and free pool) forms of Chl-*a*; k_r, k_d and k_d' are rate constants of the respective transformations.

of degradation depend on the initial form of the pigment and, when metazoan grazers are present, on digestion processes (Bianchi *et al.,* 1988). In the present study, we emphasized anoxic closed incubations as representative of a major possible degradation environment for Chl-*a* in muddy LIS sediments, where oxygen is usually absent below 1–2 mm. These incubation experiments minimized the effects of macrofaunal and meiofaunal digestion, particle reworking, and irrigation on decomposition. Nevertheless, as shown subsequently, reasonable estimates of particle mixing and organic matter flux result from models which assume that the degradation rates obtained from incubation experiments are generally typical.

The pattern of Chl-*a* degradation observed in the experiments described here was influenced by the method of extraction of Chl-*a*. The difference between total Chl-*a* extracted from previously frozen compared with fresh (never frozen) sediments, as well as the initial time dependence of extractable Chl-*a* in incubated fresh sediments, imply that at least two Chl-*a* pools can be operationally defined in LIS sediments. There apparently exists a pool that is not readily extractable by acetone but that can be released by freezing/thawing, defined as the "bound" pool. A second pool is relatively free and extractable without manipulation, defined as the "free" pool. The exact matrix association of these pools is unknown, but separation of the Chl-*a* into two pools leads to additional information about the degradation mechanisms of Chl-*a*. Relative sizes of these operational pools vary seasonally; this may be related to seasonal changes in primary productivity and hence flux to the sediments. In addition, more subtle matrix changes may be due to changes in the "binding" of Chl-*a* during various life stages of the phytoplankton cells or to changes in the dominant species present during different seasons. The differences in loss rates observed in the different Chl-*a* pools suggest that the anoxic degradation of Chl-*a* may involve at least two basic processes: Chl-*a* in the bound pool is released from cells or other binding sites (perhaps controlled by biophysical processes); and, Chl-*a* degrades in both the bound and free pools by a variety of possible pathways (Fig. 8). Both the release process and degradation of Chl-*a* may occur simultaneously. The time-dependent pattern of Chl-*a* concentration observed in incubations of fresh

material indicates that both release to the extractable pool and degradation can be described phenomenologically by first-order kinetics.

For bound Chl-*a*, the loss rate during incubation of fresh sediment is assumed to be represented by:

$$dC_b/dt = -(k_r + k'_d)C_b \tag{1a}$$

where C_b is the concentration of Chl-*a* in bound form; k_r is the apparent reaction rate constant for release of bound Chl-*a*; k'_d is the reaction rate constant for degradation of Chl-*a* within the bound pool; and t is time. This latter rate constant, k'_d, was not directly measured in the present work, but by analogy with degradation of free Chl-*a* (k_d is the reaction rate constant for degradation of free Chl-*a*), is assumed to be a first order process. Such a reaction remains to be further studied.

The initial increase of Chl-*a* concentration during incubation implies that the release process is much faster than degradation of both free and bound Chl-*a*, that is, $k_rC_b > (k'_dC_b + k_dC_f)$ where C_f is the concentration of free Chl-*a* and $C_b \leq C_f$ in general. This leads to the simplifying assumption that $k_r \gg k'_d$, giving:

$$dC_b/dt \sim -k_rC_b. \tag{1b}$$

For free Chl-*a*, the time-dependent concentrations will result from the net balance between the release of bound Chl-*a* and the degradation of free Chl-*a*. This can be represented by:

$$dC_f/dt = k_rC_b - k_dC_f. \tag{1c}$$

The time-dependent concentration of Chl-*a* measured in the incubations where samples were frozen and thawed before incubation is:

$$dC_f/dt = -k_dC_f. \tag{2}$$

Where samples were frozen before extraction but after incubation, this expression is:

$$dC_t/dt = dC_b/dt + dC_f/dt = -k_dC_f \tag{3}$$

where $C_t = C_b + C_f$. C_t is the actual measured (extracted) Chl-*a* in this case because of the freezing process. When the sample is frozen before incubation it is assumed that all Chl-*a* is converted to C_f and decomposes accordingly ($C_b = 0$). When the sample is frozen before extraction but after incubation, the measured concentration (C_t) is related directly to degradation of the free portion of the Chl-*a* pool (C_f) by simple addition of Eqs. (1b) and (1c).

The solutions to the Eqs. (1c, 2, 3) describing these various conditions are:

$$C_f = \frac{k_r(C_b)_0}{k_d - k_r}[\exp(-k_rt) - \exp(-k_dt)] + (C_f)_0 \exp(-k_dt) \tag{4a}$$

$$C_f = (C_f)_0 \exp(-k_d t) \tag{4b}$$

$$C_t = \frac{k_r(C_b)_0}{k_d - k_r}\left[\frac{k_d}{k_r}\exp(-k_r t) - \exp(-k_d t)\right] + (C_f)_0 \exp(-k_d t). \tag{4c}$$

Fitting experimental data (such as that shown in Fig. 5a and 5b) to Eq. (4a), k_r and k_d can be estimated as $k_r = 0.14$–0.19 d^{-1} and $k_d = 0.02$–0.04 d^{-1}. In calculating k_d, we assumed that C_f eventually decays entirely. This is consistent with low concentrations at depth in sediments but was not verified over the experimental timescale. When the bound Chl-*a* concentration has a magnitude similar to the free Chl-*a* concentration, the release rate is much larger than the degradation rate so that the release process dominates during the initial incubation (about 1 week). This results in an initial increase in extractable Chl-*a* concentration during the incubation of previously unfrozen, fresh sediment. After most bound Chl-*a* is released from the cells, the degradation of free Chl-*a* becomes dominant, which causes a decrease of the extractable Chl-*a* concentration. A similar case of initial increase in Chl-*a* concentration was found in chloropigment degradation studies of microbial decomposition and macrofaunal grazing on macrophytes (Bianchi and Findlay, unpublished). They attributed the initial increase in Chl-*a* concentration to extraction efficiency: some Chl-*a* may be bound in certain structural plant compounds or cells which can resist extraction by organic solvents. It is interesting to note that Bianchi and Findlay found k_d values for Chl-*a* degradation in macrophyte detritus within the range found here for LIS sediments. Moreover, the k_d values found here were also similar to those for aphotic Chl-*a* degradation in the hypolimnion (Leavitt and Carpenter, 1990).

c. Particle mixing and organic matter fluxes. Although the exact controls on Chl-*a* degradation are unknown, the documentation of the overall phenomenological rate constants allows the use of Chl-*a* concentration distributions to quantify a variety of sedimentary processes including particle reworking rates and the flux of phytoplankton debris to the sea floor. The concentration patterns of Chl-*a* with depth in sediments result from balances between supply, internal transport, and decomposition. The seasonal variation in chloropigment profiles are due to variations in the relative importance of these processes. Because the concentration of Chl-*a* decreases within a few centimeters of the sediment surface, decomposition rates must be rapid relative to sediment mixing. Assuming that Chl-*a* can be treated as a particle-associated component, its vertical distribution can be described by (e.g., Berner, 1980):

$$\frac{\partial C}{\partial t} = D_B \frac{\partial^2 C}{\partial x^2} - S\frac{\partial C}{\partial x} + \Sigma R \tag{5}$$

where:

C = Chl-*a* concentration, mass/volume of total sediment;
t = time;
x = depth in sediment;
D_B = particle mixing coefficient;
S = sedimentation rate;
ΣR = reaction term.

D_B is assumed to be constant over the sediment intervals considered here. In LIS, S ranges from 0.02 to 0.06 cm/yr while values of D_B measured using ^{234}Th in the upper few centimeters are typically in the range of 0.01 to 0.1 cm^2/day (Aller *et al.*, 1980). Given a length scale, L, of 5–10 cm, the Peclet number (SL/D_B) is much less than 1 so that the advection term can be ignored in these surface sediments (Boudreau, 1985). If the overall degradation process follows first-order kinetics as implied by the incubation experiments, then the general equation (5) can be simplified to:

$$\frac{\partial C}{\partial t} = D_B \frac{\partial^2 C}{\partial x^2} - k_d C \tag{6}$$

where k_d = degradation rate constant. Because k_r is relatively large, degradation is the rate-limiting step and thus k_d will dominate the profile shape and magnitude.

Approximating the Chl-*a* distributions as steady state on a timescale of ~1–2 months and setting the boundary conditions as:

$$x = 0, \qquad C = C_0$$
$$x \to \infty, \qquad C = C_\infty$$

the solution of the simplified equation (6) is:

$$C = (C_0 - C_\infty) \exp\left(-x\sqrt{k_d/D_B}\right) + C_\infty. \tag{7}$$

The assumption of near steady-state is allowed by the relatively rapid degradation rate and spacing of seasonal samples (see subsequent discussion). The slope of a plot of ln $(C - C_\infty)$ vs. x yields the ratio $\sqrt{k_d/D_B}$. If D_B or k_d are known independently, the remaining quantity can be calculated. In the present cases, estimates of k_d for Chl-*a* are available from the incubation experiments and D_B estimates are also available from ^{234}Th distributions measured on the same cores (Cochran *et al.*, unpublished). We chose to calculate D_B from Chl-*a* sediment distributions using an averaged, approximately temperature-independent, k_d of 0.03 d^{-1}. Values of k_d from the incubation experiments range between 0.02 and 0.04 d^{-1}. The resulting values of D_B are within a factor of 3 of those estimated from ^{234}Th profiles (Table 2). Thus, the assumptions and degradation rate used here for Chl-*a* lead to results which are at least consistent with those from interpretation of the ^{234}Th patterns; models of Chl-*a*

Table 2. Bioturbation coefficients and Chl-*a* fluxes through the sediment-water interface at LIS stations P and R. All calculations assume a degradation rate constant for Chl-*a* of 0.03 d^{-1}.

Time of sampling	D_B from chl-*a* (cm^2/d)	D_B from ^{234}Th (cm^2/d^*)	J_{chl} from I_r ($nmol/cm^2/d$)	J_{chl} from model ($nmol/cm^2/d$)
Station P				
5-17-88	0.069	0.107	0.39	0.40
8-28-88	0.182		0.05	0.06
10-26-88	0.120	0.174	0.07	0.12
2-13-89	0.003		0.18	0.19
4-25-89	0.010		0.31	0.29
Station R				
5-16-88	0.043	0.126	0.10	0.10
8-19-88	0.099	0.360	0.06	0.06
10-24-88	0.056	0.019	0.03	0.03
2-13-89	0.004		0.07	0.07
4-25-89	0.026		0.05	0.06

*From Cochran *et al.* (unpublished).

profiles may thus represent a simple alternative to radiochemical measures of particle bioturbation. Moreover, the half-life (23.1 d) of Chl-*a* in LIS sediments is very close to that of ^{234}Th (24.1 d) so that scaling in this case is nearly identical for constant source functions. Differences between D_B from Chl-*a* profiles and D_B from ^{234}Th distributions measured at the same sites may result from differences between the diffusion of organic-rich particles and the diffusion of the total particle matrix containing ^{234}Th which includes both inorganic and organic materials. Such a difference could occur as a result of selective feeding by organisms or of other processes affecting diffusion.

Calculated values of D_B are higher in summer than in winter and spring (Fig. 9), implying that benthic transport activities intensify in summer and that reactive

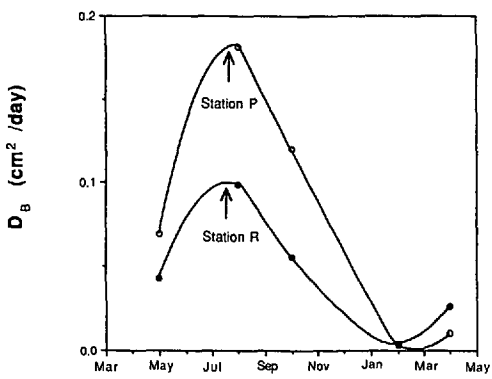

Figure 9. Seasonal pattern of D_B calculated from Chl-*a* profiles at Stations P and R. Lines are added only to aid comparison of data.

pigments are transported to deeper sediment layers (as observed in Fig. 2). The subsurface maxima of Chl-*a* observed in summer and fall (Fig. 2 and data not shown) also indicate decreasing Chl-*a* fluxes from overlying water at those times and may indicate that Chl-*a* is being mixed down into the sediment through 'conveyor-belt' feeding (Boudreau, 1986; Rice, 1986; Robbins, 1986). Depth-dependent decomposition may also play an unknown role in producing the Chl-*a* maxima. The low D_B in winter reflects lower temperatures and generally decreased metabolic activity. Changes in D_B with season at station P (shallow) are larger than at station R (deeper). D_B values at station P and R are similar in winter and spring (low), while D_B at station P is distinctly larger than that at station R in summer and fall. These observations agree with relative spatial and temporal patterns in D_B values derived from ^{234}Th distributions (Aller *et al.*, 1980; Cochran *et al.*, unpublished), but provide a greater degree of seasonal resolution than previous measurements. The differences in D_B between station P and R are likely related to community distributions and feeding behaviors of benthos at the two sites.

The 'steady state' flux, J, of Chl-*a* across the sediment-water interface can be estimated from the measured profiles and the transport/reaction model by two methods. One method uses Fick's law (Berner, 1980) and reflects both the transport model and reaction kinetics:

$$J = (C_O - C_\infty)\sqrt{k_d D_B} \tag{8}$$

where $(C_o - C_\infty)$ is the reactive or labile concentration of Chl-*a* at the sediment-water interface. A second method simply balances total supply and decomposition rates:

$$J = k_d I_r = k_d \int_0^\infty (C - C_\infty)dx \sim k_d \sum_n (C - C_\infty)_n L_n \tag{9}$$

where I_r is the inventory of reactive Chl-*a* over the sediment sample interval, L_n. These methods are truly independent only if measures of D_B and k_d are independently available from ^{234}Th distributions and from Chl-*a* incubations, respectively. Seasonal variations in calculated fluxes are shown in Figure 10. The values of Chl-*a* fluxes from the two methods are very close in the present case except for station P during Oct, 1988 (Table 2) when a Chl-*a* maximum occurs and the simple steady-state model cannot describe this behavior. These approximate calculations ignore seasonal dependence of k_d due to temperature, effects of nonsteady state J on I_r, effects of oxic diagenesis, and the effects of digestion, mixing, and irrigation by benthos.

Order-of-magnitude uncertainties in calculations of J and D_B resulting from the simple assumption of "local" steady state can be estimated using more complex, realistic time-dependent boundary conditions for Chl-*a* inputs. The estimated fluxes (Eq. 8, 9; Fig. 10) suggest that a regular, periodic flux boundary condition is a better

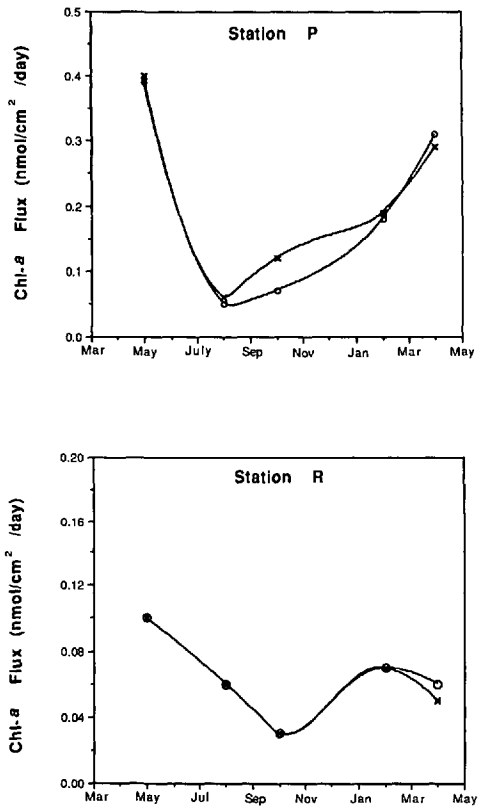

Figure 10. Seasonal pattern of Chl-*a* fluxes to the sea floor at Station P and R. Lines are added only to aid comparison of data. (o) J_{chl} from inventory; (x) J_{chl} from model.

but not exact approximation to reality. Assuming that:

$$J = \bar{J} + \Delta J \sin(\omega t) \tag{10}$$

where $\bar{J}$ is an average flux and ΔJ the amplitude of oscillation at frequency ω, then the inventory is (e.g. Wollast, 1986):

$$I_r = \frac{\bar{J}}{k_d} + \frac{\Delta J}{\sqrt{k_d^2 + \omega^2}} \sin(\omega t - \delta) \tag{11a}$$

$$\delta = \cos^{-1}\left(\frac{k_d}{\sqrt{k_d^2 + \omega^2}}\right) \tag{11b}$$

These equations indicate that our use of Eq. (9) to estimate fluxes from inventories is likely to underestimate the amplitude of seasonal variation by the factor $k_d/\sqrt{k_d^2 + \omega^2}$ (Eq. 11a) and to have a phase lag of order δ (Eq. 11b). In the present cases with $k_d \sim 0.03\ d^{-1}$ and $\omega \sim 0.017\ d^{-1}$ ($2\pi\ yr^{-1}$), use of the simple equation (9) underestimates

the amplitude by ~14% and has a phase lag of ~30 days. This order of error seems acceptable given the relatively few samples we have to resolve the true seasonal flux pattern and the uncertainty in k_d (see Fig. 10).

It can be shown from the analytical solution to Eq. (6) assuming the periodic surface boundary condition of Eq. (10), that in the range of k_d and ω values under consideration:

$$\frac{\partial \ln C}{\partial x} \approx -\sqrt{\frac{k_d}{D_B}} - \frac{\Delta J}{\bar{J}} \alpha \sin\left(\frac{\delta}{2}\right) \cos\left[\omega t - x\alpha \sin\left(\frac{\delta}{2}\right) - \frac{\delta}{2}\right] \tag{12a}$$

where

$$\alpha = \sqrt{\frac{\sqrt{k_d^2 + \omega^2}}{D_B}}. \tag{12b}$$

The term $x\alpha \sin(\delta/2)$ is small so the gradient in ln C is nearly constant with depth. Eq. (12) demonstrates that if the flux varies periodically, our simple method of calculating D_B from the depth gradient in ln C would result in an apparent periodic oscillation of D_B even if D_B were actually constant. The phase shift of the oscillation is smaller than the inventory phase shift (11a) (and slightly depth dependent), but the sign of the amplitude is such that an apparent maximum in our calculated D_B occurs roughly during the time of minimum flux (e.g., early fall). In the present cases the oscillation amplitude of D_B about its mean value is likely overestimated by ~25–40% and the apparent phase shifted slightly toward the fall. Again, we consider this order of uncertainty acceptable in the present context.

The Chl-*a* flux estimates can be converted to estimates of phytoplankton carbon flux to the sea floor by using an average C_{org}/Chl-*a* ratio of 60 for phytoplankton. For LIS, this ratio ranges between 50 and 70 depending on water depth and season (Tantichodok, 1989). We can compare phytoplankton carbon fluxes estimated from Chl-*a* with organic carbon fluxes independently derived from oxygen fluxes measured during short-term incubation of sediment cores (Mackin *et al.*, unpublished). This comparison shows a generally linear agreement between the two estimates (Fig. 11). The ratio between phytoplankton carbon flux and carbon equivalent O_2 flux calculated from this data is approximately 0.54. Several factors could explain why this ratio is less than 1. The "local" steady state approximation (Eq. 9) underestimates periodic (or pulsed) fluxes by ~14% (Eq. 11). Other labile organic carbon sources exist in addition to primary production (e.g., river input, runoff) in LIS sediments which would lower the ratio. Also, using the C_{org}/Chl-*a* ratio for phytoplankton in this calculation may underestimate carbon flux since the ratio in particles reaching the sediment will likely be higher due to decomposition of Chl-*a* in the water column. It is also possible that the degradation rate model used is oversimplified. Regardless, the agreement between the two types of estimates is remarkably close and implies

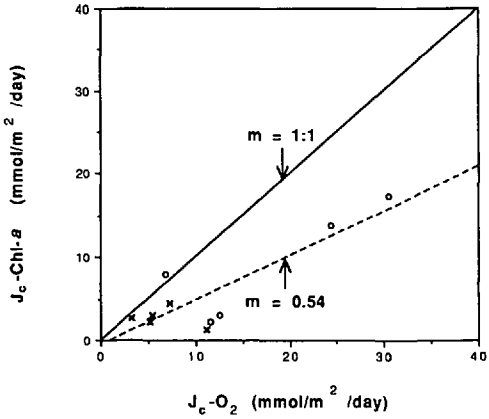

Figure 11. Comparison between phytoplankton carbon fluxes estimated from the Chl-*a* degradation model described here and organic carbon equivalent fluxes derived from O_2 fluxes (Mackin *et al.*, unpublished; $C/O_2 = 0.77$ reaction ratio assumed). Measurements were made at the same time. The dashed line is a linear regression of the data with a slope of 0.54, $r^2 = 0.743$. The solid line has a slope of 1.0. (o) Station P data; (x) Station R data.

that Chl-*a* inventories/flux estimates may be good alternatives to sediment trap estimates of labile benthic C supply in shallow water. The ratios during summer and fall are generally lower than those in spring, reflecting the seasonal pattern of primary production.

5. Conclusions

The distribution of Chl-*a* in Long Island Sound sediments reflects the delivery of plankton debris, decomposition, and particle reworking. Concentrations generally decrease exponentially within a few centimeters below the sediment-water interface due to decomposition processes. Incubation experiments were designed to study the processes controlling the loss of Chl-*a* from sediments. Two pools of Chl-*a* were operationally defined as "free" or "bound" according to their extractability by freeze-thaw techniques. The loss of Chl-*a* from fresh sediment may involve at least two basic processes: the release of bound Chl-*a* (which may be controlled by biophysical processes) and the degradation of free Chl-*a* into phaeopigments or colorless residues (which may be controlled by biochemical reactions). Mathematical models suggest that the release rate constant ($k_r = 0.14$–0.19 d^{-1}) is larger than the degradation rate constant ($k_d = 0.02$–0.04 d^{-1}). An assumption used in these models is that the degradation rate constant for Chl-*a* in the bound state is insignificant relative to the release rate constant from the bound state.

Profiles of Chl-*a* in LIS sediments suggest that decomposition rates of Chl-*a* are faster than surface sediment mixing rates. These profiles can be quantitatively modeled and estimates of both particle mixing rate and fluxes of Chl-*a* to the bottom

can be made. Carbon fluxes calculated from Chl-*a* distribution agree within a factor of 2 or better with those necessary to support oxygen fluxes to the sea floor. Values of mixing coefficients, D_B, calculated from Chl-*a* profiles and diagenetic models of decomposition, are roughly comparable with those estimated from ^{234}Th distributions from the same area (generally within a factor of 2–4). Relatively shallow station P has higher surface mixing rates than the deeper station R, likely due to differences in benthic animal distribution and feeding behavior at the two sites.

Acknowledgments. We would like to thank Captain H. Stuebe and B. Zielenski for help with sampling during all cruises. We are grateful to J. K. Cochran, J. E. Mackin, E. M. Cosper, and T. S. Bianchi, who kindly provided access to unpublished data and manuscripts. We also thank D. Repeta for useful discussions and comments on the manuscript. This research was supported by EPA National Estuaries Program (Long Island Sound Study) and NSF Grant OCE 86-13688 to R. C. A. and NSF 87-10765 to C. L. This is contribution number 805 of the Marine Sciences Research Center, SUNY.

REFERENCES

Aller, R. C. 1980. Diagenetic processes near the sediment-water interface of Long Island Sound. I. Decomposition and nutrient element geochemistry (S, N, P). Adv. Geophys., *22,* 237–350.

Aller, R. C. and L. K. Benninger. 1981. Spatial and temporal patterns of dissolved ammonium, manganese, and silica fluxes from bottom sediments of Long Island Sound, U.S.A. J. Mar. Res., *39,* 295–314.

Aller, R. C., L. K. Benninger and J. K. Cochran. 1980. Tracking particle associated processes in nearshore environments by use of $^{234}Th/^{238}U$ disequilibrium. Earth Planet. Sci. Lett., *47,* 161–175.

Aller, R. C. and J. K. Cochran. 1976. $^{234}Th/^{238}U$ disequilibrium in nearshore sediment: particle reworking and diagenetic time scales. Earth Planet Sci. Lett., *20,* 37–50.

Aller, R. C. and J. Y. Yingst. 1980. Relationships between microbial distributions and the anaerobic decomposition of organic matter in surface sediments of Long Island Sound, USA. Mar. Biol., *56,* 29–42.

Banta, G. T., J. Tucker, A. E. Giblin and J. E. Hobbie. 1990. Seasonal patterns of benthic respiration and nitrogen mineralization in Buzzards Bay, Massachusetts: Importance of temperature and organic matter. EOS, *71,* 111.

Berner, R. A. 1980. Early Diagenesis: A Theoretical Approach, Princeton Univ. Press, 241 pp.

Bianchi, T. S., R. Dawson and P. Sawangwong. 1988. The effects of macrobenthic deposit-feeding on the degradation of chloropigments in sandy sediments. J. Exp. Mar. Biol. Ecol., *122,* 243–255.

Bianchi, T. S. and S. Findlay. 1991. Decomposition of Hudson River macrophytes: Photosynthetic pigment transformations and decay constants. Estuaries, *14,* 65–73.

Boudreau, B. P. 1986. Mathematics of trace mixing in sediments: I. Spatially-dependent, diffusive mixing. Am. J. Sci., *286,* 161–198.

Cole, J. J., S. Honjo and N. Caraco. 1985. Seasonal variation in the flux of algal pigments to a deep-water site in the Panama Basin. Hydrobiologia, *122,* 193–197.

Conover, S. A. M. 1956. Oceanography of Long Island Sound, 1952–1954. IV. Phytoplankton. Bull. Bingham Oceanogr. Collect., *15,* 62–112.

Downs, J. N. 1989. Implications of the phaeopigment, carbon and nitrogen content of sinking particles for the origin of export production. Ph. D. dissertation, University of Washington.

Furlong, E. T. and R. Carpenter. 1988. Pigment preservation and remineralization in oxic coastal marine sediments. Geochim. Cosmochim. Acta, *52,* 87–99.

Gelder, S. R. and W. E. Robinson. 1980. Identification of phaeopigments in the digestive gland of *Mytilus edulis* L. by microspectrofluorometry. J. Exp. Mar. Biol. Ecol., *43,* 281–292.

Graf, G. 1989. Benthic-pelagic coupling in a deep-sea benthic community. Nature, *341,* 437–439.

Hallegraeff, G. M. 1981. Seasonal study of photoplankton pigments and species at a coastal station off Sydney: importance of diatoms and the nanoplankton. Mar. Biol., *61,* 107–118.

Hawkins, A. J. S., B. L. Bayne, R. F. C. Mantoura and C. A. Llewellyn. 1986. Chlorophyll degradation and absorption throughout the digestive system of the blue mussel *Mytilus edulis* L. J. Exp. Mar. Biol. Ecol., *96,* 213–223.

Jeffrey, S. W., and G. M. Hallegraeff. 1987. Chlorophyllase distribution in ten classes of phytoplankton: a problem for chlorophyll analysis. Mar. Ecol. Prog. Ser., *35,* 293–304.

Keely, B. J. and R. G. Brereton. 1985. Early chlorin diagenesis in a recent aquatic sediment. Org. Geochem., *10,* 975–980.

Leavitt, P. R. and S. R. Carpenter. 1990. Aphotic pigment degradation in the hypolimnion: Implications for sedimentation studies and paleolimnology. Limnol. Oceanogr., *35,* 520–534.

Mackin, J. E. and K. T. Swider. 1989. Organic matter decomposition pathways and oxygen consumption in coastal marine sediments. J. Mar. Res., *47,* 681–716.

Mantoura, R. F. C. and C. A. Llewellyn. 1983. The rapid determination of algal chloropyll and carotenoid pigments and their breakdown products in natural waters by reversed-phase high-performance liquid chromatography. Anal. Chim. Acta, *151,* 297–314.

McCall, P. L. 1977. Community patterns and adaptive strategies of the infaunal benthos of Long Island Sound. J. Mar. Res., *35,* 221–266.

—— 1978. Spatial-temporal distributions of Long Island Sound infauna: The role of bottom disturbance in a nearshore marine habitat, *in* Estuarine Interaction, M. L. Wiley, ed., 191–219. Academic Press, New York.

Montagna, P. A., J. E. Bauer, D. Hardin and R. B. Spies. 1989. Vertical distribution of microbial and meiofaunal populations in sediments of a natural coastal hydrocarbon seep. J. Mar. Res., *47,* 657–680.

Rabalais, N. N. and R. E. Turner. 1990. Louisiana continental shelf sediments: Pigments and biogenic silica. EOS, *71,* 70.

Ramm, A. E. and D. A. Bella. 1974. Sulfide production in anaerobic microcosms. Limnol. Oceanogr., *19,* 110–118.

Repeta, D. J. and R. B. Gagosian. 1987. Carotenoid diagenesis in recent marine sediments—I. The Peru continental shelf (15°S, 75°W). Geochim. Cosmochim. Acta, *51,* 1001–1009.

Rice, D. L. 1986. Early diagenesis in bioactive sediments of New England: Relationships between the diagenesis of Beryllium-7, sediment reworking rates, and the abundance of conveyor-belt deposit feeders, *Scolopolos* spp. (Orbiniidae: Polychaeta). J. Mar. Res., *44,* 149–184.

Riley, G. A. 1956. Oceanography of Long Island Sound, 1952–1954. II. Physical oceanography. Bull. Bingham Oceanogr. Collect., *15,* 15–46.

Robbins, J. A. 1986. A model for particle-selective transport of tracers in sediments with conveyor-belt deposit feeders. J. Geophys. Res., *91,* 8542–8558.

Shuman, F. K. and C. J. Lorenzen. 1975. Quantitative degradation of chlorophyll by a marine herbivore. Limnol. Oceanogr., *2,* 580–586.

SooHoo, J. B. and D. A. Keifer. 1982. Vertical distribution of phaeopigments. I. A simple grazing and photooxidative scheme for small particles. Deep-Sea Res., *29,* 1539–1551.

Tantichodok, P. 1989. Relative importance of phytoplankton and organic detritus as food sources for the suspension-feeding bivalve, *Mytilus Edulis* L., in Long Island Sound, Ph. D. dissertation, State University of New York at Stony Brook.

Turekian, K. K., J. K. Cochran, L. K. Benninger and R. C. Aller. 1980. The sources and sinks of nuclides in Long Island Sound, *in* Estuarine Physics and Chemistry: Studies in Long Island Sound, B. Saltzman, ed., 129–164, Academic Press, New York.

Yingst, J. Y. and D. C. Rhoads. 1978. Seafloor stability in central Long Island Sound. Part II. Biological interactions and their potential importance for seafloor erodibility, *in* Estuarine Interaction, M. N. Wiley, ed., 245–260, Academic Press, New York.

Wakeham, S. G. and C. Lee. 1991. Production, transport, and alteration of particulate organic matter in the marine water column, *in* Organic Geochemistry, M. H. Engel and S. A. Macko, ed., Plenum Press. (in press).

Welschmeyer, N. A. and C. L. Lorenzen. 1985. Chlorophyll budgets: Zooplankton grazing and phytoplankton growth in a temperate fjord and the Central Pacific Gyres. Limnol. Oceanogr., *30,* 1–21.

Wollast, R. 1986. Basic concepts in geochemical modeling, *in* The Role of Air-Sea Exchange in Geochemical Cycling, P. Buat-Menard, ed., 1–34, D. Reidel Publ. Co., Dordrecht Holland.

Woodwell, G. M. and E. V. Pecan. 1973. Flax Pond: An estuarine marsh. Brookhaven National Laboratory, BNL 50397, Upton, New York.

Received: *5 July, 1990;* revised: *26 March, 1991.*